Modeling and Control of a Magnetic Levitation System

By: Marwan K. Abbadi

Advisor: Dr. Winfred Anakwa

Date: May 13, 2004

Department of Electrical and Computer Engineering-Bradley University

ABSTRACT

Magnetic levitation technology has been receiving increasing attention because it helps eliminate frictional losses due to mechanical contact. Some engineering applications include high-speed maglev trains, magnetic bearings and high-precision platforms. The objectives of this project are to model and control a laboratory-scale magnetic levitation system. The control algorithm is implemented using assembly language on Intel 8051 microprocessor to levitate and stabilize a spherical steel ball at a desired vertical position.

TABLE OF CONTENTS

1. INTRODUCTION

Overview

Magnetic levitation (or maglev) systems are electromechanical devices that suspend ferromagnetic materials using electromagnetism. Maglev technology has been receiving increasing attention since it eliminates energy losses due to friction. Centered on friction reduction, maglev systems have wide engineering applications such as magnetic bearings, high-precision positioning platforms, aerospace shuttles, and fast maglev trains.

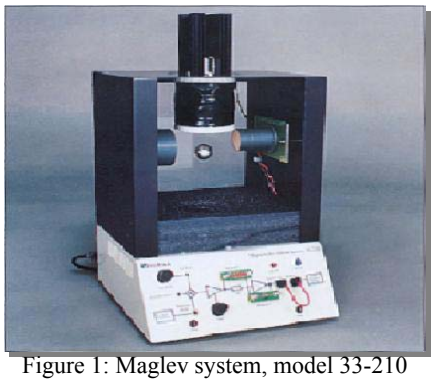

Figure 1: Maglev system, model 33-210

Problem Definition

Maglev systems, based on electromagnetism, are characterized by open-loop instability and nonlinear dynamics that suggest the need of stabilizing controllers.

The Electrical and Computer Engineering Department (ECE) has purchased a laboratory-scale maglev system from Feedback Limited Inc, shown in figure 1. The maglev system included an analog controller that levitated and stabilized a set of hollow steel balls about an operating region. However, there is little insight known about the model of the plant. After consulting with the project advisor, we agreed upon the following project objectives:

1. To obtain a good model for the maglev system, model 33-210 manufactured by Feedback Limited In.

2. To implement a microcontroller-based digital controller that stabilizes a 21-gram steel ball and tracks reference input signals applied to the maglev.

2. SYSTEM DESCRIPTION

The control system consists of three inputs and one output. The inputs are:

1. Set point – adjusts the vertical position of the ball.
2. Reference input signal
3. Disturbances – such as power supply fluctuations, coil temperature variations and external forces applied to the ball. The final output of the system is the actual ball position. Figure 2 shows a block diagram of the digital controller interfaced to the maglev system.

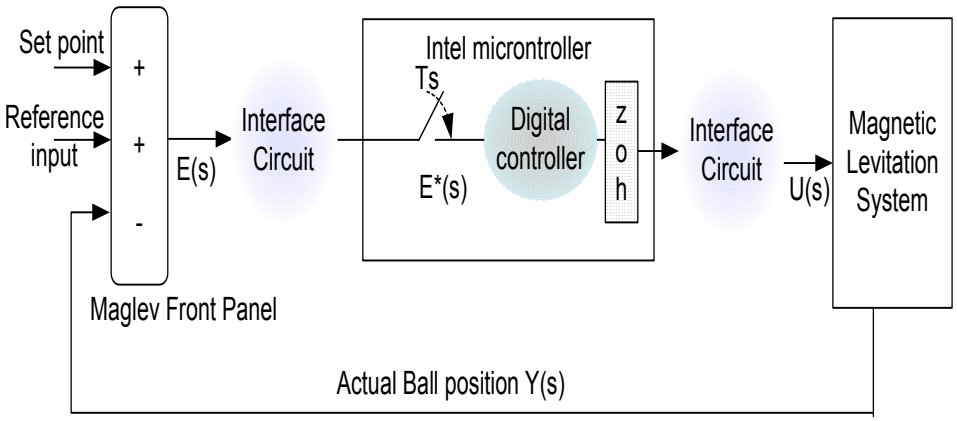

Figure 2: Overall system block diagram

3. SYSTEM IDENTIFICATION

A fundamental concept in science and technology is that of mathematical modeling. System identification is conducted to obtain the plant transfer function needed for the control design. Once a good model is obtained and verified, a suitable control law can be implemented to compensate the plant instability and improve performance.

Analytical Model

Analytical and experimental plant models were obtained for comparison and verification. According to T. H. Wong, laboratory-scale maglev systems are represented with electrical and mechanical equations [1]. Figure 3 shows the RLC coil circuit that displaces the steel ball using electromagnetism.

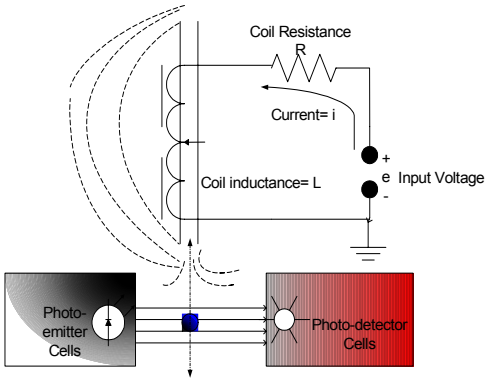

Figure 3: Coil circuit

Using Kirchoff's voltage rule around the loop, the electrical equation is:

$$e = R \cdot i + L\frac{\delta i}{\delta t} - L_0 \cdot x_0 \frac{i}{x^2}\frac{\delta x}{\delta t} \qquad (1)$$

Where:

e= coil voltage i= coil current R= coil resistance L=coil inductance x=ball position xo and Lo are nominal operating constants.

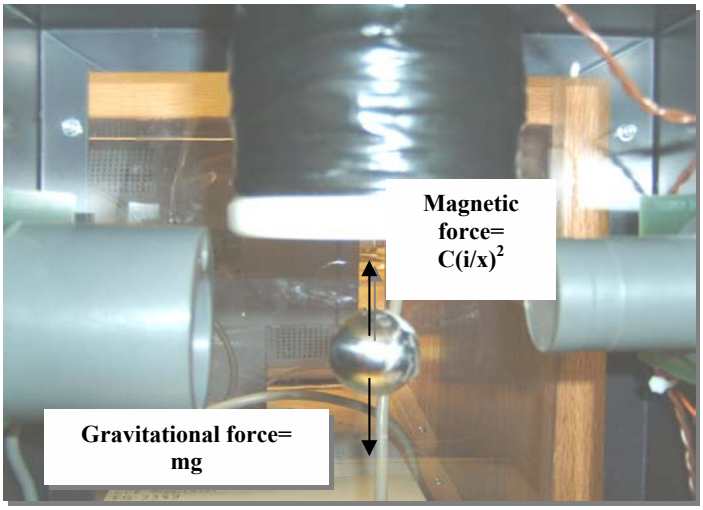

Figure 4: Force diagram

On the other hand, the mechanical equation is obtained from the force diagram based on Newton's second law, as shown in figure 4:

$$F = GF - EF = m \cdot g - C \cdot \left(\frac{i}{x}\right)^2 \qquad (2)$$

Where

C= Magnetic constant determined experimentally=1.477×10^{-4} $N.m^2/A^2$

m= mass of steel ball= 0.021 kg

g= gravitational acceleration= 9.82 m/s^2

Using Taylor series expansion to *linearize* the non-linear differential equations about the equilibrium point xo=22.5 mm, the plant analytical model is:

$$Gp(s)_{analytical} = \frac{0.0013}{(s/29.14+1)(s/29.14-1)(s/70.15+1)} \qquad (3)$$

It was determined that the coil circuit was driven by an active circuit that indictates that the current ***i*** is a non-linear function of the coil voltage ***e***.

Experimental approach

Obtaining and fitting frequency response data to estimate a plant model is a common practice in control design. Closed-loop frequency response data for the plant were obtained and plotted in the bode diagram shown in figure 5.

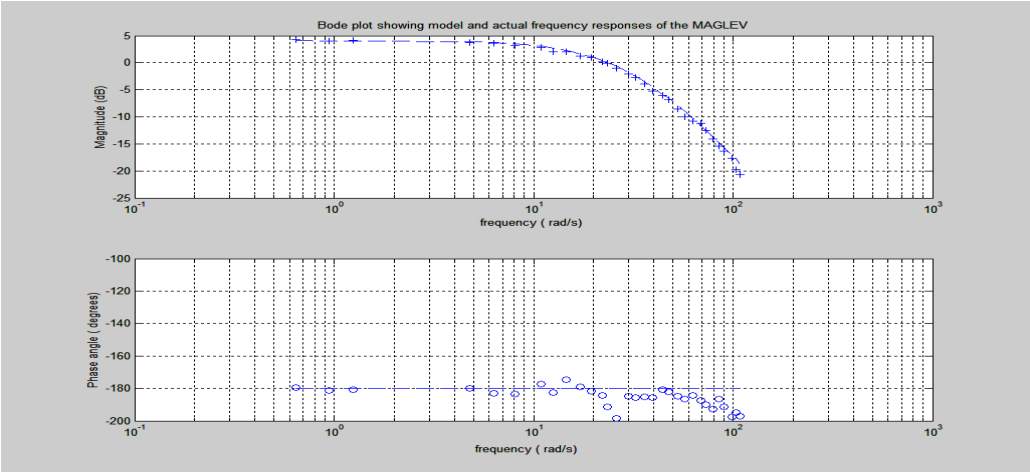

Figure 5: Frequency response data for the plant

From the diagram, the experimental model of the maglev system was approximated as:

$$G_{p\_\exp}(s) = \frac{1.60}{(s/30.5 + 1)(s/30.5 - 1)} \qquad (4)$$

The experimental model was used rather than the analytical one because it is more accurate since it represents the practical model of the system.

4. CONTROLLER IMPLEMENTATION

The analog controller from the manufacturer was *discretized* and implemented on a microcontroller to examine the performance of the same control law using analog and digital realizations. This approach would reveal the effect of *discretization* on the plant performance.

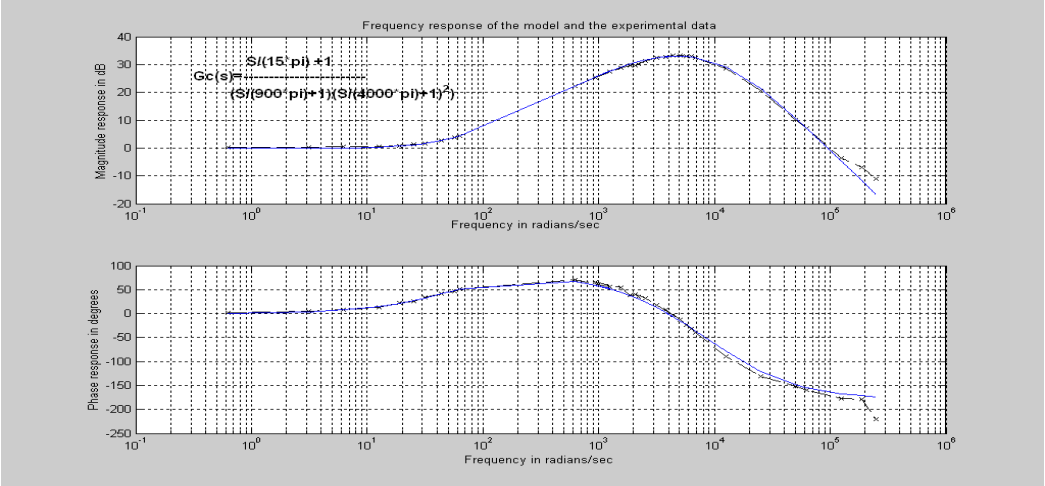

Figure 6: Frequency response data for controller from manufacture

From frequency response plot shown on figure 6, the analog controller from the manufacturer was approximated as:

$$G_{c\_man}(s) = \frac{\frac{s}{15\pi}+1}{(\frac{s}{900\pi}+1)(\frac{s}{4000\pi}+1)^2} \qquad (5)$$

The double poles at -4000π rad/s are relatively higher than the plant bandwidth of 126 rad/s. Ignoring the high-frequency poles, the analog controller model was simplified to a first-order model:

$$G_{c\_man}(s) = \frac{\frac{s}{15\pi}+1}{(\frac{s}{900\pi}+1)} \qquad (6)$$

Sampling frequency

After conducting frequency response analysis, the cut-off frequency was approximated to 126 rad/s. According to Franklin/Powell rule, the sampling

frequency must be at least six times the cut-off frequency [2]. To satisfy this heuristic rule, the sampling period cannot be slower than 8.3 ms. Different sampling periods were examined and a sampling frequency of 5 ms resulted in the most stable and satisfactory tracking system response.

Discretization

The analog controller was transformed to a digital equivalent using bilinear transformation with a sampling period of 5 ms. The transfer function of the digital controller is:

$$G_C(z) = \frac{8.3 - 6.56 \cdot z^{-1}}{1 + 0.7521 \cdot z^{-1}} \qquad (7)$$

To avoid software overflow, the transfer function was normalized to:

$$G_C(z) = 8.3 \frac{1 - 0.7904 \cdot z^{-1}}{1 + 0.7521 \cdot z^{-1}} \qquad (8)$$

The gain of 8.3 was implemented in hardware, and the normalized digital filter was implemented on the microcontroller.

5. HARDWARE

In addition to the controller gain implementation, hardware circuitry was needed to adjust the signals before and after the microcontroller as shown in figure 2. The hardware circuitry must:

a. Adjust the error signal before being sent to the microcontroller.

b. Provide impedance matching between the hardware interface and the plant.

c. Adjust the control signal to the correct scale.

d. Amplify the control signal from the microcontroller to the maglev.

e. Filter high-frequency noise and provide anti-aliasing filtering.

Error-to-A/D

The error signal was level-shifted to a range of 0~5V that corresponds to the 80515 microcontroller voltage rating. The interface circuitry scales down the error signal by a factor of 1/2 and provides a 2.5 V offset as shown in figure 7. The hardware components and layout for the circuit is shown in appendix B, figure 17a.

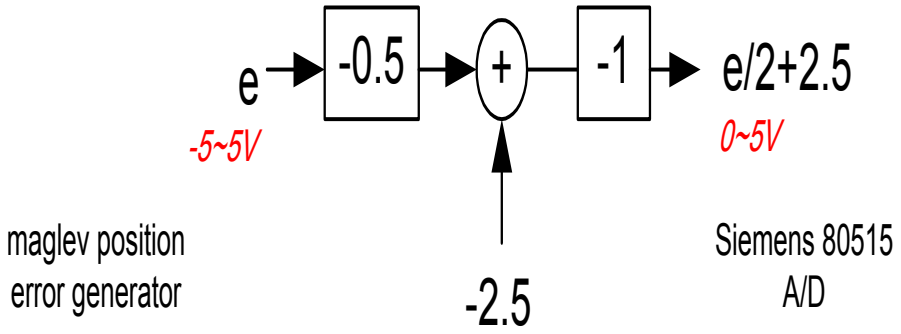

Figure 7: Error-to-A/D shifter

Impedance Matching

A voltage follower was connected between the final control signal and the maglev system. This solves possible impedance mismatch thereby ensuring enough voltage and current drive the maglev system.

D/A-to-Control

The factored control signal sent from the microcontroller needed to be readjusted to the correct scale and amplified by a controller gain of 8.3. Figure 8 shows a signal flow diagram between the microcontroller and the maglev system. The hardware components and layout is shown in appendix B, figure 17b.

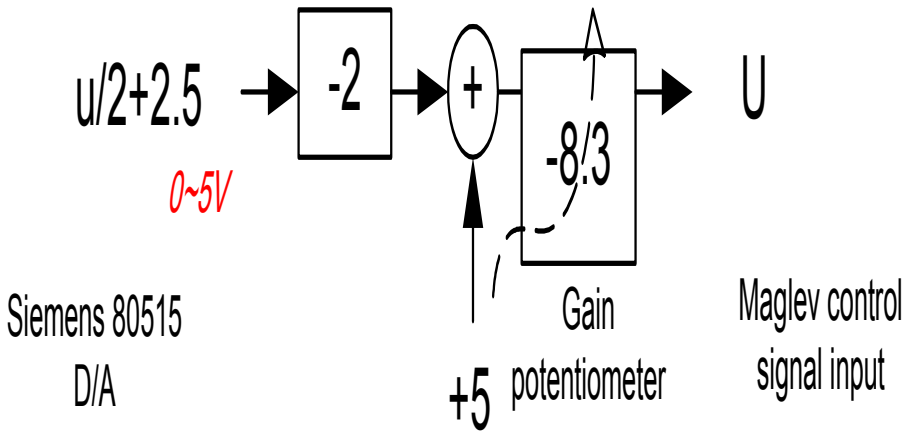

Figure 8: D/A-to-Control shifter

Anti-aliasing/noise-reduction filter

Anti-aliasing filters are important key elements in digital control. Apart from reducing aliasing and distortion of the sampled signals, they are used to filter out high-frequency noise that can burn the microcontroller chip. A first-order, low-pass filter was connected to the final control signal to eliminate any amplified noise. This ensures less noise at the final stage before the control signal reaches the maglev system. The pole of the filter was placed at 188 rad/s. The RC circuit is connected at the end terminal of the D/A-to-Control circuit as shown in figure 17b.

6. SOFTWARE

The software code of the project was programmed using assembly language on an 80515 microcontroller manufactured by Siemens. The software code was developed using *Keil uvision 2* simulation package.

The primary tasks of the software:

a. sample and decode the error signal

b. compute the corresponding control signal

c. encode then produce the control signal through the D/A.

Decoding and encoding scheme

The decoding and encoding scheme controlled the polarity of the signals by defining signed number representation. Signed number representation was needed since positive and negative signals were sampled and produced via the analog and digital converters. Table 1 displays specific error values and their mapped sample value.

Initial error signal	Adjust error signal to EMAC
5	5 =(255d)
0	2.5=(127d)
-5	0=(0)

Table 1: Error values mapping

The microcontroller samples the error signal through an 8-bit A/D channel. Then, the error signal is checked if it is greater than 127 (2.5V) or not. If it is greater than 127, then the error signal is positive and the sign bit is cleared and vice versa.

When the control signal is computed, it is divided by 2 and added to 127 thereby generating u/2+2.5 which is sent to the D/A, as shown in figure 8. This solves the polarity problem and ensures the resultant control signal is within the 0~5V range of the D/A.

Realizing the mathematical function on 8051microcontroller

The 80515 microcontroller does not handle floating-point arithmetic, which suggests extra steps are needed to represent the coefficients shown in equation 8. The coefficients were approximated using fixed-point rational integers.

From equation (8), the recursive equation of the factored control law is:

$$U(n) = E(n) - \langle 0.7521 \cdot E(n-1) + 0.7904 \cdot U(n-1) \rangle \qquad (9)$$

Approximating to fixed-point realization:

$$U(n) = E(n) - \langle \frac{10}{14} \cdot E(n-1) + \frac{11}{14} \cdot U(n-1) \rangle \qquad (10)$$

The remainders of the division operation were truncated in the mathematical computations because they only affect the first or second least significant bits. This error can be simply ignored because the 80515 has +/- 1 to 2 least-significant bits error during sampling and generation of signals using the 8-bit A/D and D/A respectively.

Software flowchart

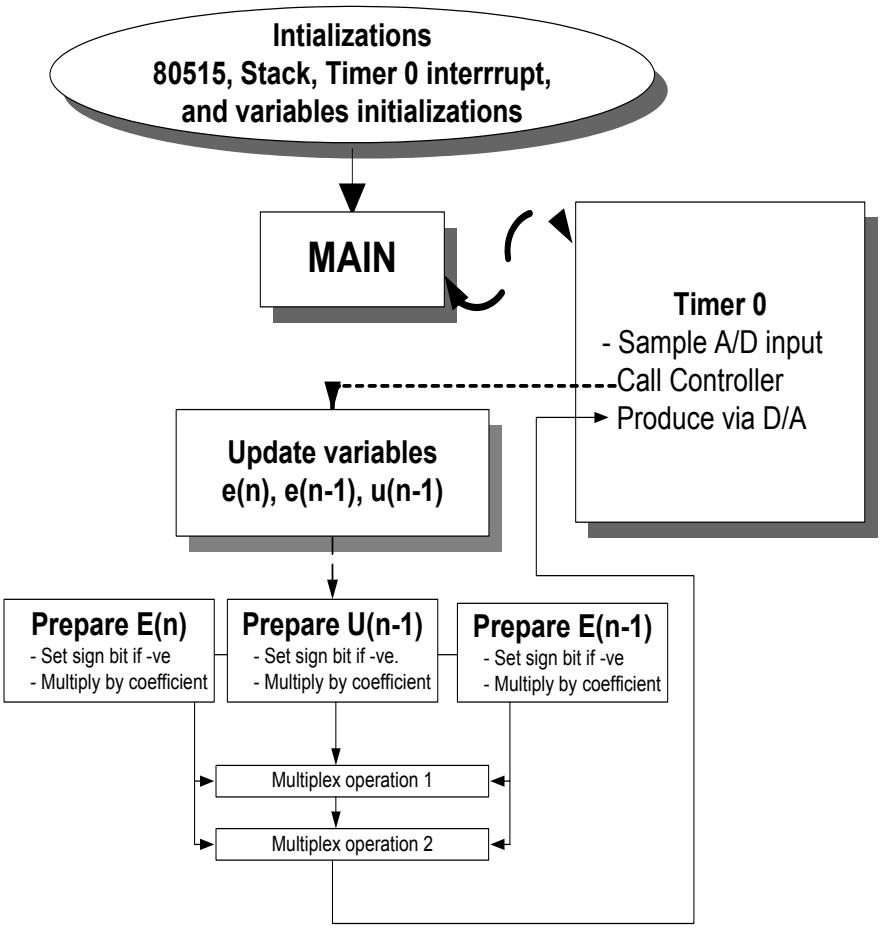

Figure 9: Software flow chart

Figure 9 shows the software flowchart for the project. Initially, the program initializes different parameters such as timer interrupt, stack pointer, 80515 port initializations and initial conditions of the control signals. The main program is a dummy loop that waits for the timer to overflow every 5 ms.

When the timer interrupt handler is serviced, the error signal is sampled and stored in the accumulator. The program calls the controller subroutine to compute the corresponding control signal based on the value of the accumulator.

At the beginning of the controller subroutine, the current error e(n), past error e(n-1), and past control u(n-1) signals are updated. Next, the polarity of a signal is determined and accordingly a sign bit is set or cleared. Using the same 2's complement convention for sign bits, if the number is negative then the sign bit is set, otherwise cleared. The signals are then multiplied by their corresponding coefficients through series of division and multiplications instructions before they are sent to the arithmetic operations routine.

According to the combination of the different sign bits of the operands, the appropriate arithmetic operation is selected. If both signals were positive, the result is positive and addition operation is executed. Similarly, if both signals were negative, the result is negative and addition operation is also performed. The final control signal is computed and adjusted through the encoding/decoding scheme and sent out via the D/A. The D/A generates the control signal and the operation is repeated every 5 ms.

7. RESULTS AND ANALYSIS

Stability

The 21-gram steel ball was stabilized at the equilibrium point xo=22.5 mm from the electromagnet. Figure 10 shows the ball response at steady-state with no reference input applied.

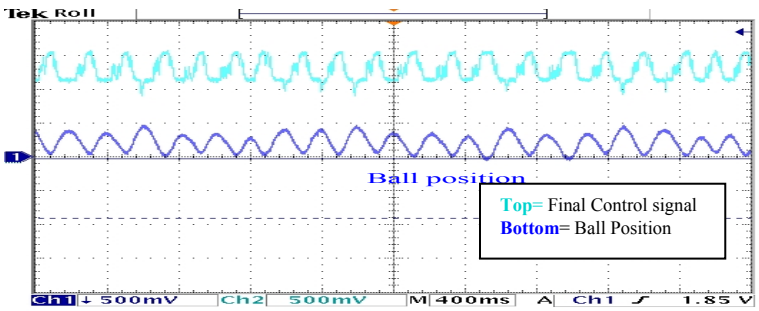

Figure 10: Ball response at steady state

As shown in figure 10, there were small oscillations in the ball position that were due to quantization, truncation and computation errors of the 8-bit microcontroller. A/D and D/A quantization errors are the primary reason for these oscillations rather than the computational errors. Figure 11 shows the ball position along with the factored control signal from the microcontroller. As shown from figure 11, the quantization errors occur every sampling period and peak to a value of + 100 and -50 mV. These values correspond to +5 and – 2 least-significant bit that are then amplified resulting in the position waveform shown.

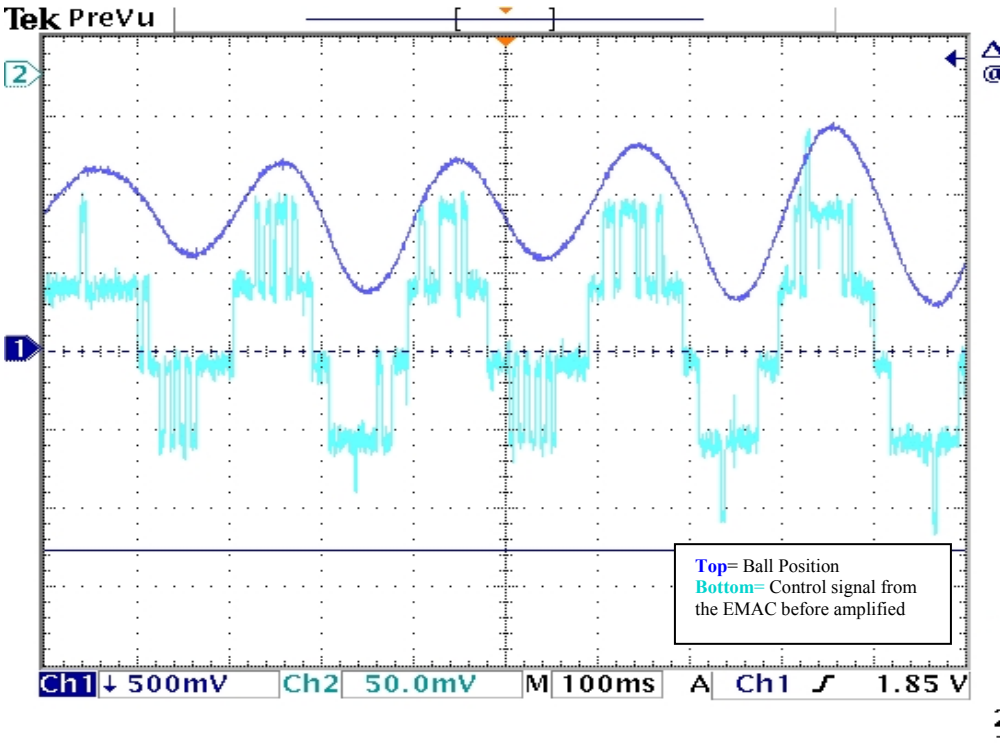

Figure 11: Factored control signal from the microcontroller zoomed out to display quantization errors.

Tracking

The ball tracked sinusoidal, square and triangular reference inputs with a magnitude less than 0.4 V. The tracking performance was not very good because of the oscillations, however using higher-resolution converters will produce better tracking results. Figure 12 shows the response of the ball position to a sinusoidal reference input. Apart from the oscillations, the ball position tracks the reference input signal with constant error because the controller equation produces a non-zero steady-state position error. As shown in figure 12, the response peaks at the same instance as the reference input.

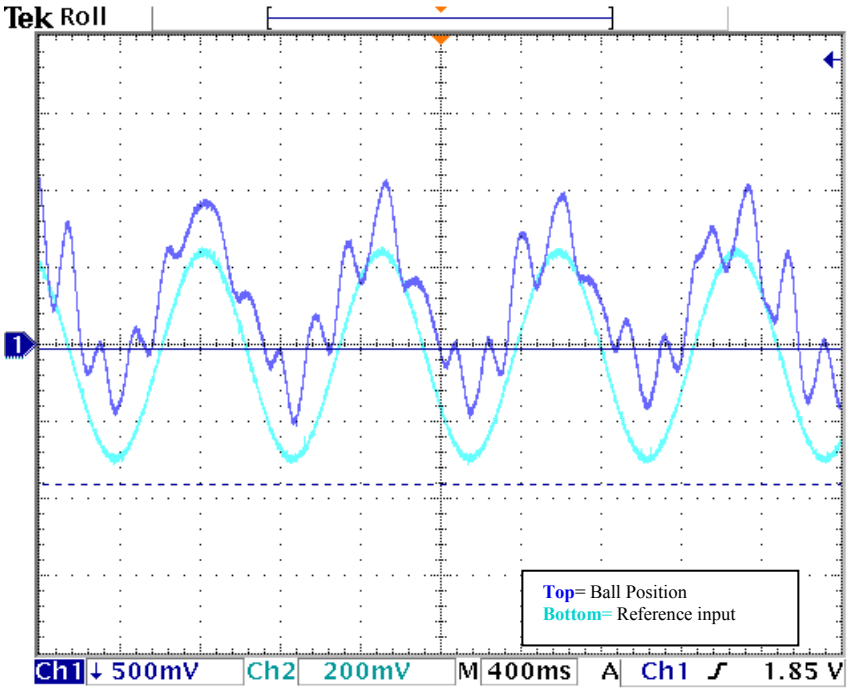

Figure 12: Sinusoidal input response

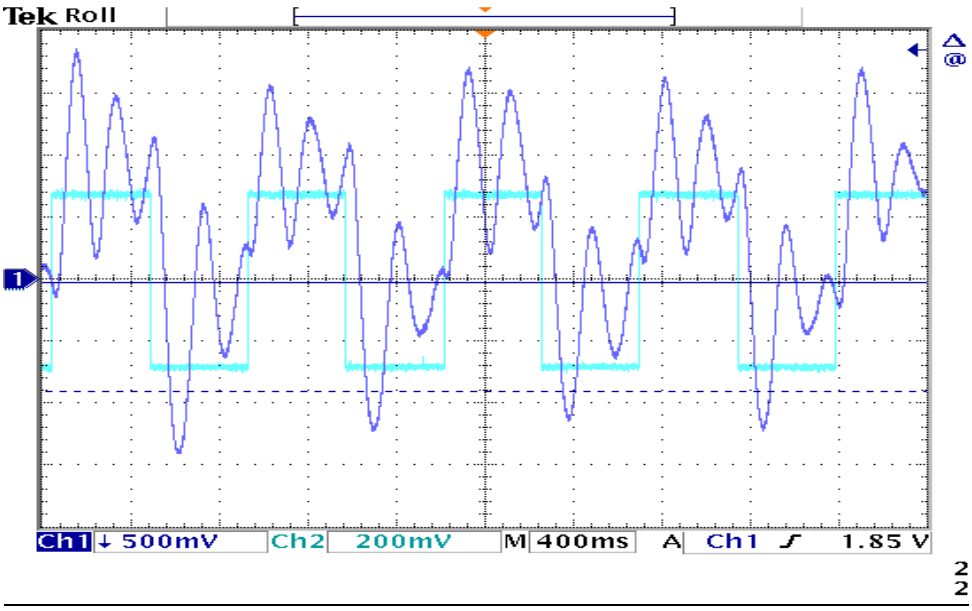

Figure 13: Square wave response

Figure 13 shows the response of the ball position to a square wave reference input. As seen in the figure, the ball position attempts to track the reference signal and gradually reduces the error.

Step response

Simulation and experimental step responses of the analog and digital controller are shown in figures 14. Figure 14a shows the closed-loop step response using the analog controller from the manufacturer. The response is inverted because the ball position in the maglev front panel is inverted; however the actual response is positive.

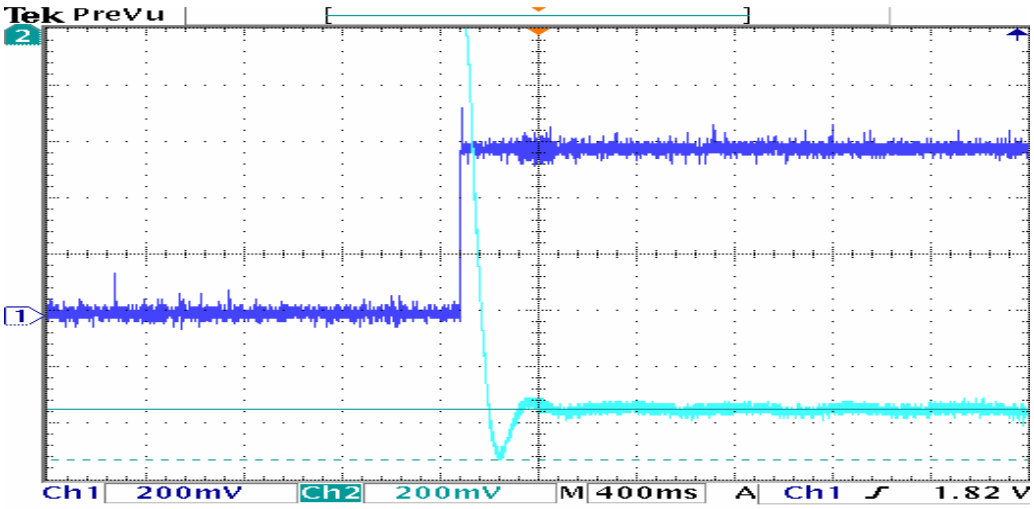

Figure 14a: CL response for 0.6V step input with controller from manufacturer connected.

Figure 14b shows the closed-loop step response from SIMULINK with the analog controller connected. There was 0.2V difference, however the overall responses are similar.

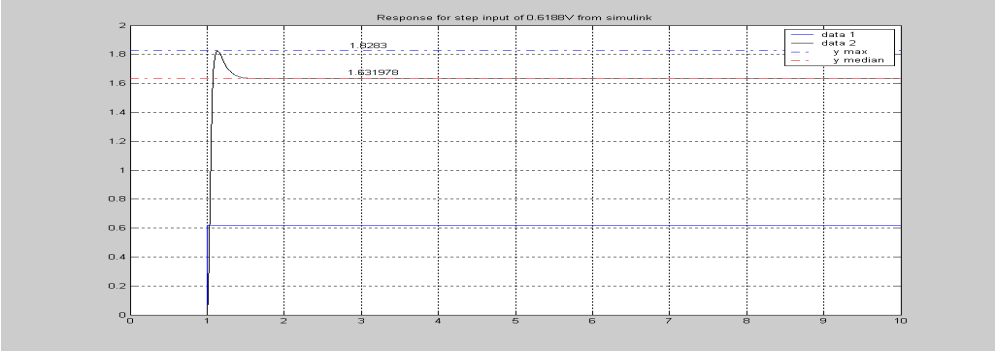

Figure 14b: CL response for 0.6V step input from SIMULINK for the analog controller

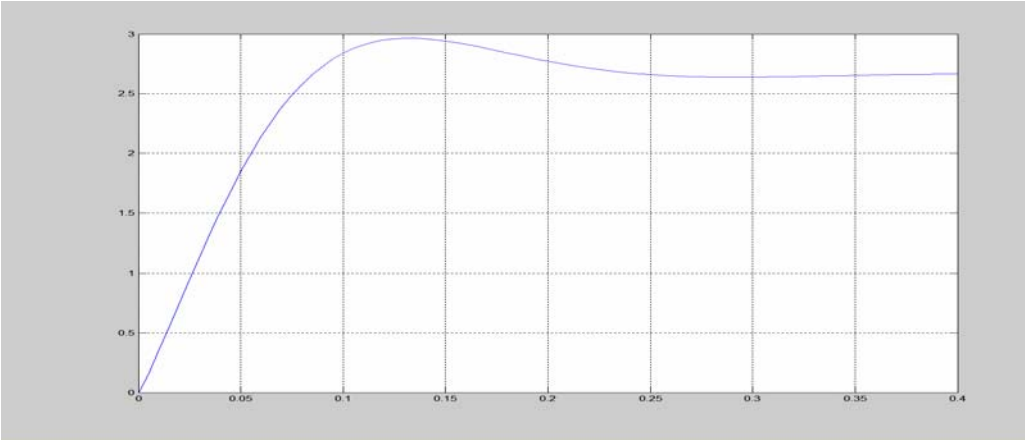

Figure 14c: SIMULINK CL step response with digital controller

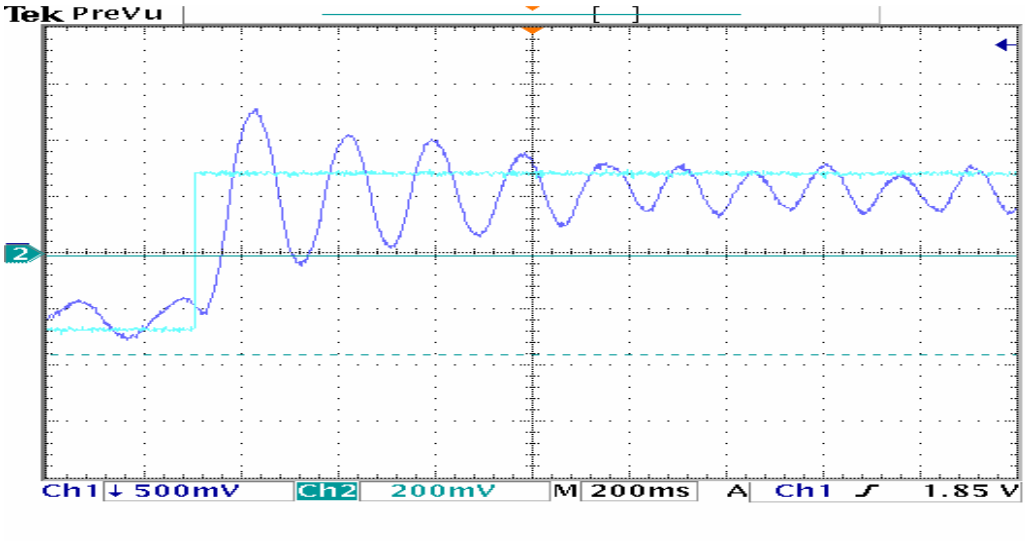

Figure 14d: CL step response for the digital controller

Figure 14c and 14d show the simulations and experimental step response with the digital controller connected. In figure 14d, the digital controller overshoots as expected and tries to minimize the error. At steady state, the response continued to oscillate due to the quantization errors discussed earlier.

8. PARTS AND EQUIPMENT

Quantity	Description
1	Maglev system from Feedback Inc, model 33-210
1	200 MHz PC with Keil software package to develop and run the software code
1	80515 Microcontroller from Siemens with built-in A/D and D/A
3	HP power supplies
1	Tube-caliber for measuring distance in millimeter range
7	LM741 operational amplifiers

9. CONCLUSIONS

This project investigated different control practices that are common in control systems design. Modeling a non-linear, open-loop unstable plant, such as maglev systems and inverted pendulums, is a challenging engineering problem. The project examined the different approaches in obtaining a model for the maglev system.

Another practice in control systems is investigating performance of different controllers such as analog vs. digital. The analog controller from the manufacturer was converted to digital equivalent using bilinear transformation with a sampling frequency of 5ms.

Different phenomena associated with sampled data systems were observed during the interface of the microcontroller. This includes effect of varying the sampling period, quantization errors, aliasing and programming low resolution microcontrollers. Assembly language was used rather than C language because C compiler is needed for C language which can add more costs to the project.

10. ACKNOWLEDGMENTS

I would like to thank Dr. W. Anakwa for his continuous support and advice during the different stages of the project. Special thanks are due to Mr. David Miller for supplying the tube-caliber needed during the modeling stage for adjusting the ball position.

11. REFERENCES

[1] Wong, T. H. "Design of a magnetic levitation system-an undergraduate project," *IEEE Tran. on Education*, vol E-29, no. 4, November 1986.

[2] Franklin, Powell & R.D Harbor, *Feedback Control of Dynamic Systems, 3rd Ed.* Addison-Wesley 1994.

12. APPENDICES

APPENDIX A: Modeling plots

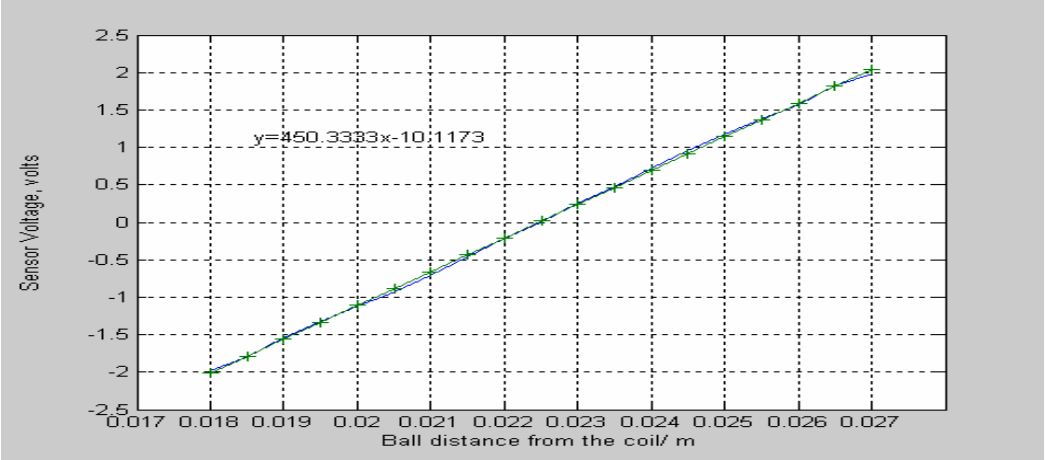

Figure 15 Sensor Calibration (gain=450.3V/m)

Figure 15 shows the sensor calibration data obtained during the modeling phase. The sensor gain was determined to be 450.3 V/m.

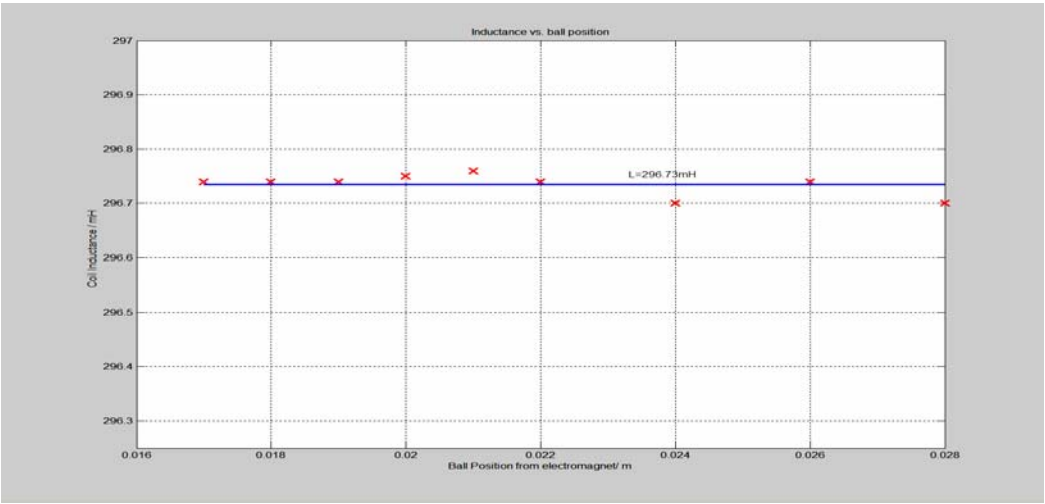

Figure 16: Coil inductance vs. ball position,
L=constant=296.73mH

Figure 16 shows the coil inductance at different ball positions. In the region of operation, the coil inductance was approximated as a constant equal to 296.73mH.

APPENDIX B: Hardware circuits

Error-to-A/D

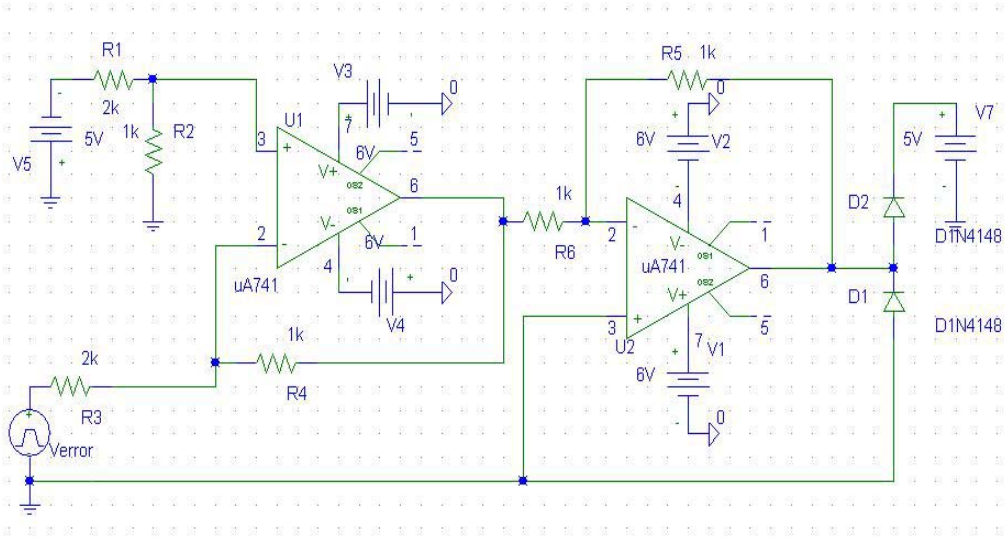

Figure 17a: Error-to-A/D circuitry

Figure 17a shows the level-shifter circuitry needed to adjust the error signal. The two diodes at the end terminal provide protective circuitry that limits voltages above 5.5V and less than -0.5V to be sent to the microcontroller.

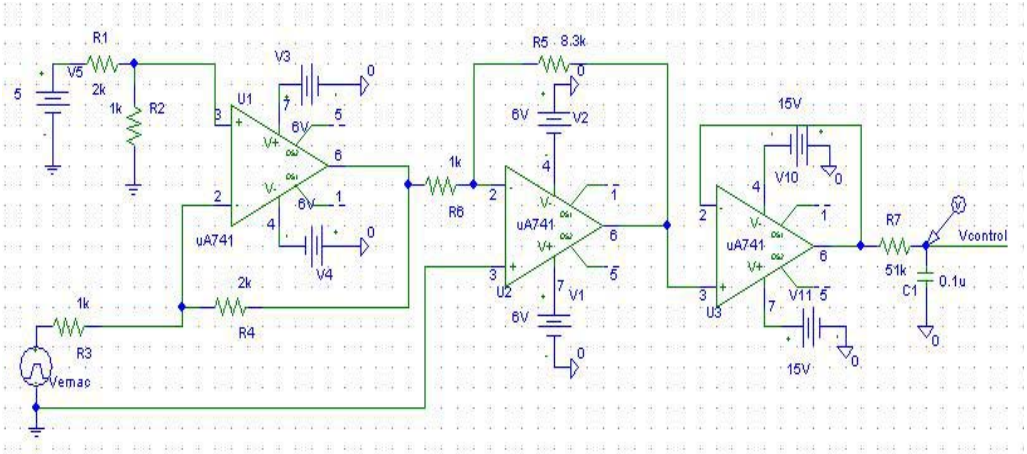

Figure 17b: D/A-to-Control

Figure 17b shows the interface circuitry needed to amplify and readjust control signal. A low-pass filter is connected at the end terminal to filter high-frequency noise and provide anti-aliasing filtering effect.